Supporting Online Material for

Porphyrin-based supramolecular nanofibres as a dynamic and activatable photosensitiser for photodynamic therapy

Nicolás M. Casellas,[a,b] Gaole Dai,[c] Evelyn Y. Xue,[c] M. Jesús Vicente-Arana,[d] Dennis K. P. Ng,*[c] Tomás Torres*[a,b] and Miguel García-Iglesias*[a,b,e]

[a] Department of Organic Chemistry, Universidad Autónoma de Madrid (UAM), Institute for Advanced Research in Chemical Sciences (IAdChem), Calle Francisco Tomás y Valiente, 7, 28049 Madrid, ES. [b] IMDEA Nanociencia, c/ Faraday 9, Campus de Cantoblanco, 28049, ES. [c] Department of Chemistry, The Chinese University of Hong Kong, Shatin, N.T., Hong Kong, China. [d] Servicio Interdepartamental de Investigación, Facultad de Ciencias, UAM. [e] QUIPRE Department, Nanomedicine-IDIVAL, Universidad de Cantabria, Avd. de Los Castros, 46, 39005 Santander, Spain.

Contents

Experimental Details

1. Materials

Chemicals were purchased from commercial suppliers (SIGMA Aldrich and Alfa Aesar) and used without further purification unless stated otherwise. All solvents were of AR quality and purchased from either Scharlab or Carlo Erba. Dry THF was degassed and obtained after passing through an activated alumina column in a solvent purification system. Water was purified using an EMD Milipore Mili-Q integral water purification system. Column chromatography was carried out on silica gel (Merk, kieselgel 60, 230-400 mesh, 60 Å). Size exclusion chromatography was carried out on Biorad Biobeads SX-1 (200-400 mesh). Reactions were followed by thin-layer chromatography on aluminum sheets precoated with 0.25 mm 60-F254 silica gel from Merck. All reactions were performed under an atmosphere of dry argon unless stated otherwise. Compound **1** was synthesised according to the our previously described procedure.[1]

2. Methods

^{1}H-NMR and ^{13}C-NMR spectra were recorded on a Bruker AC-300 or a Bruker AC-500 spectrometer. Chemicals shifts are given in ppm (δ) values relative to tetramethylsilane (TMS). Splitting patterns are labelled as s, singlet; d, doublet; dd, doublet of doublet; t, triplet; q, quartet; quin, quintet; m, multiplet and b stands for broad. Matrix-assisted laser desorption/ionisation time-of-flight (MALDI-TOF) mass spectra were recorded on a Bruker Reflex III instrument that was equipped with a nitrogen laser operated at 337 nm and recorded in the positive-ion mode. High-resolution mass spectra were acquired using a 9.4 T IonSpec QFT-MS FT-ICR mass spectrometer. The samples were analysed with a hybrid analyser QTOF model MAXIS II of Bruker. An ACQUITY UPLC system from the commercial house Waters was used as an entryway in the flow injection analysis mode.

Ultraviolet-visible (UV-Vis) absorption spectra and fluorescence spectra were recorded on a Jasco V-660-spectrophotometer and a Jasco FP-8600 spectrofluorometer respectively, both with a Jasco Peltier ETCS-761 temperature controller incorporated. The measurements were performed using quartz cuvettes (1 cm). Solutions were prepared by weighting the necessary amount of sample for a given concentration. Water solutions were prepared by injecting a concentrated DMSO solution (1 x 10^{-2} M) into water milli-Q to obtain the desired final concentration. In all cases, the solutions were optically transparent.

For transmission electron microscopy (TEM) study, 5 μL of sample was deposited on carbon film-coated copper grids (200 mesh; Beijing Zhongjingkeyi Technology Co. Ltd) and

air-dried before the TEM images were taken using a FEI Tecnai G2 Spirit transmission electron microscope operated at 120 kV acceleration voltage.

3. Solvent-dependent (SD) model [2]

The Gibbs free energy of monomer association (ΔG), the parameter *m*, that relates the ability of the good solvent to interact with the monomer, and the cooperativity degree (σ) have been derived by using the SD model[2] (Fig. 3 d-f in the main text). The application of eqn (1) – (3) allows the derivation of the complete set of thermodynamic parameters associated with the supramolecular polymerisation mechanism of **Por(PEG)$_4$** (Table 1 in the main text).

$$\Delta G^{'} = \Delta G + mf \quad (1)$$

$$\Delta G^{'} = -RTlnK_e \quad (2)$$

$$\sigma = K_n/K_e \quad (3)$$

4. Analysis of HDX-MS measurements[3]

Hydrogen/deuterium exchange (HDX) experiments followed by mass spectrometry measurements were carried out using a Maxis II QTOF mass spectrometer (Bruker) equipped with an electrospray source. The instrumental parameters were set as follows: Mass range: 600-3500 Da, capillary voltage: 3.4 kV, dry temperature: 200 ° C, nebuliser pressure (N_2) : 0.3 bar and dry gas flow (N_2) : 4.0 mL/min. **Por(PEG)$_4$** samples were diluted from a H_2O solution 5.0 x 10^{-3} M with D_2O (including 7.5 μM NaI to facilitate the detection) to a concentration of 5.0 x10^{-4} M. These samples were aliquoted at different times and HRMS analysis was acquired in the positive detection mode. The sample solutions were introduced into the spectrometer with a Harvard syringe pump (11 Plus, Harvard Apparatus) at a flow rate of 10 μL/min. All samples were stored at room temperature during the course of the experiment. Before the HDX-MS measurements, the system was calibrated with a solution of phosphazene in acetonitrile (Agilent Technologies). Each measurement was averaged over 1 minute to account for the instabilities in the signal.

All HDX-MS experiments were performed under similar conditions and at room temperature. In all cases the distributions with triple sodium ions were used for the calculations.

Two aspects were taken into account for the calculation of the percentage of deuterated analogues of **Por(PEG)$_4$** during the experiments:

a. Correction for the presence of isotopes overlapping with deuterated molecules.
b. Correction for H/D exchange due to the presence of H_2O.

a) Correction for the presence of isotopes overlapping with deuterated molecules.

By diluting a **Por(PEG)$_4$** sample in D_2O, all the hydrogen atoms of the OH groups on the periphery and the outermost amide groups were instantly replaced by deuterium atoms leading to the immediate transformation to **Por(PEG)$_4$**-4D. It was assumed that only the hydrogen atoms of the OH groups exchanged immediately. For **Por(PEG)$_4$** peaks corresponding to **Por(PEG)$_4$**-1D, **Por(PEG)$_4$**-2D, **Por(PEG)$_4$**-3D, **Por(PEG)$_4$**-4D, **Por(PEG)$_4$**-5D, **Por(PEG)$_4$**-6D, **Por(PEG)$_4$**-7D, **Por(PEG)$_4$**-8D, **Por(PEG)$_4$**-9D, **Por(PEG)$_4$**-10D, **Por(PEG)$_4$**-11D, **Por(PEG)$_4$**-12D, **Por(PEG)$_4$**-13D and **Por(PEG)$_4$**-14D, they can be distinguished after dilution into D_2O. A peak corresponding to **Por(PEG)$_4$**-0D could not be observed. All peaks observed have isotopes that overlap with the different deuterated species.

Table 1. Theoretical isotopic distribution for the triply charged species of **Por(PEG)$_4$**-14D calculated with the Bruker Compass IsotopePattern software. This would be the isotope distribution for the fully deuterated **Por(PEG)$_4$**.

m/z	Int. Relativa
954,8086	1,00
955,143	1,68
955,4774	1,49
955,8117	0,92
956,146	0,44
956,4803	0,17
956,8146	0,06
957,1489	0,02
957,4832	0,01

The theoretical isotope distribution of the fully deuterated **Por(PEG)$_4$** is given in Table 1and should be maintained taking into account that the *m*/*z* of the Por (PEG) 4mD isotopes overlaps with the *m*/*z* of Por $(PEG)_4$ (m + 1)D, by $(PEG)_4$ (m + 2)D and by $(PEG)_4$(m + 3)D... Therefore, the contribution of the Por $(PEG)_4$mD isotope must be subtracted from the measured intensity of the corresponding peaks to correct for the intensity of the isotope overlap. Based on the discussion above, Por(PEG) 4mD% can be calculated using the following equations:

$$I_{PORPEG_{1D_c}} = I_{948.48}$$

$$I_{PORPEG_{2D_c}} = I_{949.14}$$

$$I_{PORPEG_{3D_c}} = I_{949.81}$$

$$I_{PORPEG_{4D_c}} = I_{950.48}$$

$$I_{PORPEG_{5D_C}} = I_{951.14} - 1.68 \cdot I_{PORPEG_{4D_c}}$$

$$I_{PORPEG_{6D_c}} = I_{951.81} - 1.49 \cdot I_{PORPEG_{4D_c}}$$

$$I_{PORPEG_{7D_C}} = I_{952.48} - 0.92 \cdot I_{PORPEG_{4Dc}}$$

$$I_{PORPEG_{8D_C}} = I_{952.14} - 0.44 \cdot I_{PORPEG_{4D_c}}$$

$$I_{PORPEG_{9Dc}} = I_{952.81} - \left(0.18 \cdot I_{PORPEG_{4D_c}} + 1.68 \cdot I_{PORPEG_{8D_C}}\right)$$

$$I_{PORPEG_{10D_C}} = I_{953.48} - 1.49 \cdot I_{PORPEG_{8D_c}}$$

$$I_{PORPEG_{11D_c}} = I_{954.14} - (0.92 \cdot I_{PORPEG_{8D_c}} + 1.68 \cdot (I_{PORPEG_{10D_c}} - 1.44 \cdot I_{PORPEG_{8D_c}})$$

$$I_{PORPEG_{12D_C}} = I_{954.81} - (0.44 \cdot I_{PORPEG_{8D_c}} + 1.49 \cdot (I_{PORPEG_{10Dc}} - 1.44 \cdot I_{PORPEG_{8Dc}})$$

$$I_{PORPEG_{13Dc}} = I_{955.48} - (0.17 \cdot I_{PORPEG_{8D_c}} + 0.91 \cdot (I_{PORPEG_{10D_c}} - 1.44 \cdot I_{PORPEG_{8D_c}})$$

$$I_{PORPEG_{14D_c}} = I_{956.14} - (0.44 \cdot I_{PORPEG_{8D_c}} + (I_{PORPEG_{10D_c}} - 1.44 \cdot I_{PORPEG_{8D_c}} \cdot I_{PORPEG_{10D_c}})$$

b) Correction for H/D exchange due to the presence of H2O.

The presence of H_2O in the sample after tenfold D_2O dilution leads to the exchange of deuterium atoms back to hydrogen atoms, which would result in an over-estimation of the percentage of less deuterated molecules. To correct for the presence of water, the molar percentage of H_2O should be calculated first:

$$\text{mol\%}H_2O = \frac{V_{H_2O} \times \rho_{H_2O} \times M_{H_2O}}{V_{H_2O} \times \rho_{H_2O} \times M_{H_2O} + V_{D_2O} \times \rho_{D_2O} \times M_{D_2O}} \times 100\%$$

with V_{H_2O} and V_{D_2O} the volume of the aqueous sample and the volume of D_2O used to induce the H/D exchange, respectively, ρ_{H_2O} and ρ_{D_2O} the density of H_2O and D_2O, respectively, and M_{H_2O} and M_{D_2O} the molar mass of H_2O and D_2O, respectively. We have used the following constants: $\rho_{H_2O} = 1.0$, $\rho_{D_2O} = 1.1$, $M_{H_2O} = 18.01$ and $M_{D_2O} = 20.02$.

The **Por(PEG)$_4$** derivatives have 14 labile hydrogen atoms in total that can undergo H/D exchange. The relative contribution of a **Por(PEG)$_4$** molecule with r of the maximum 14 deuterium atoms exchanged to hydrogen atoms can be calculated with:

$$\binom{14}{r} \times \left(\frac{\text{mol\%}H_2O}{100}\right)^r \times \left(1 - \left(\frac{\text{mol\%}H_2O}{100}\right)\right)^{14 - r}$$

The following distributions can be calculated for **Por(PEG)$_4$**-14D in a **Por(PEG)$_4$** sample that tenfold (10.0 mol% of H_2O) diluted:

Table 2. Relative occurrence of **PorPEG$_4$** with r of the possible 14 deuterium atoms exchanged for hydrogen atoms for 10.0 mol% of H_2O in the sample after dilution into D_2O.

r	Corresponding PorPEG4	Relative occurrence for 10.0 mol% H_2O
0	PorPEG$_4$-14D	1
1	PorPEG$_4$-13D	1.00
2	PorPEG$_4$-12D	8,57x10^{-1}
3	PorPEG$_4$-11D	4.52x10^{-1}
4	PorPEG$_4$-10D	9.08x10^{-2}
5	PorPEG$_4$-9D	9.52 x10^{-3}
6	PorPEG$_4$-8D	1.06x10^{-4}
7	PorPEG$_4$-7D	1.18x10^{-6}
8	PorPEG$_4$-6D	1.31x10^{-8}
9	PorPEG$_4$-5D	1.46x10^{-10}
10	PorPEG$_4$-4D	1.62x10^{-12}
11	PorPEG$_4$-3D	1.80x10^{-14}
12	PorPEG$_4$-2D	2.01x10-^{16}
13	PorPEG$_4$-1D	2.23x10^{-18}
14	PorPEG$_4$-0D	2.48x10^{-20}

The **PorPEG$_4$** samples were diluted tenfold with D_2O, so the molar percentage of H_2O is calculated to be 10.0%. The intensity without artefacts can then be calculated with:

$$I_{PORPEG_{1D}} = I_{PORPEG_{1D_c}} - 2.48 \times 10^{-18} I_{PORPEG_{14D_c}} - 4.08 \times 10^{-2} I_{PORPEG_{4D_c}}$$

$$I_{PORPEG_{2D}} = I_{PORPEG_{2D_c}} - 2.01 \times 10^{-16} I_{PORPEG_{14D_c}} - 4.04 \times 10^{-2} I_{PORPEG_{4D_c}}$$

$$I_{PORPEG_{3D}} = I_{PORPEG_{3D_c}} - 1.80 \times 10^{-14} I_{PORPEG_{14D_c}} - 4.04 \times 10^{-2} I_{PORPEG_{4D_c}}$$

$$I_{PORPEG_{4D}} = I_{PORPEG_{4D_c}} - 1.62 \times 10^{-12} I_{PORPEG_{14D_c}} + \left(4.08 \times 10^{-2} + 4.04 \times 10^{-2}\right) I_{PORPEG_{4D_c}}$$

$$I_{PORPEG_{5D}} = I_{PORPEG_{5D_c}} - 1.46 \times 10^{--10} I_{PORPEG_{14D_c}}$$

$$I_{PORPEG_{6D}} = I_{PORPEG_{6D_c}} - 1.31 \times 10^{-8} I_{PORPEG_{14D_c}}$$

$$I_{PORPEG_{7D}} = I_{PORPEG_{7D_c}} - 1.18 \times 10^{-6} I_{PORPEG_{14D_c}}$$

$$I_{PORPEG_{8D}} = I_{PORPEG_{8D_c}} - 1.06 \times 10^{-4} I_{PORPEG_{14D_c}}$$

$$I_{PORPEG_{9D}} = I_{PORPEG_{9D_c}} - 9.52 \times 10^{-3} I_{PORPEG_{14D_c}}$$

$$I_{PORPEG_{10D}} = I_{PORPEG_{10D_c}} - 9.08 \times 10^{-2} I_{PORPEG_{14D_c}}$$

$$I_{PORPEG_{11D}} = I_{PORPEG_{11D_c}} - 4.52 \times 10^{-1} I_{PORPEG_{14D_c}}$$

$$I_{PORPEG_{12D}} = I_{PORPEG_{12D_c}} - 8.57 \times 10^{-1} I_{PORPEG_{14D_c}}$$

$$I_{PORPEG_{13D}} = I_{PORPEG_{13D_c}} - 1 I_{PORPEG_{14D_c}}$$

$$I_{PORPEG_{14D}} = I_{PORPEG_{14D_c}} + \left(1.80 \times 10^{-14} + 1.62 \times 10^{-12} + 1.46 \times 10^{-10} + 1.31 \times 10^{-8} + 4.52 \times 10^{-2} + 4.52 \times \right) I_{PORPEG_{14D_c}}$$

The percentage of deuterated analogues can be calculated:

$$\%\text{Por(PEG)4nD} = \frac{I_{\text{Por(PEG)4nD}}}{\sum_{k=1}^{14} I_{\text{Por(PEG)kD}}} \times 100\%$$

3.1 Bi-exponential fits details

The plot of the HDX percentage of Por(PEG)$_4$-14D versus time was plotted with a bi-exponential growth function with Origin 2018. The pre-defined function '*ExpGro2*' was used for the fit:

$$y = y0 + A_{fast}\exp\left(\frac{x}{t_{fast}}\right) + A_{slow}\exp\left(\frac{x}{t_{slow}}\right)$$

being y the dependent variable (percentage of deuterated molecules), x the independent variable (time) and y_0, A_{fast}, A_{slow}, t_{fast}, and t_{slow} the variables during the bi-exponential fitting. y_0 can be related to the maximum percentage of deuterated molecules that can be reached, A_{fast} and A_{slow} describe the contribution of the fast and slow component and t_{fast} and t_{slow} describe the time constants of the fast and slow component. The rate constants, k, were calculated from the time constants with:

$k_{fast} = 1/t_{fast}$ and $k_{slow} = 1/t_{slow}$

Statistical F-tests were used to confirm that the bi-exponential growth function was a better fit than a mono-exponential or tri-exponential growth function. The fits were compared pairwise (mono-exponential *vs* bi-exponential and bi-exponential *vs* tri-exponential) with the null-hypothesis being that the fit with the lowest number of parameters was the best fit.[2]

The pre-defined bi-exponential growth function was modified to include the following constraints:

$y0 \leq 100$

$y0 \geq A1 + A2$

With the bi-exponential function and constraints the following fits were found:

$$\text{Por(PEG)4} - 6D = 85.75 - 60.0\, e^{\frac{t}{-0.33}} - 22.5\, e^{\frac{t}{-2.84}} \text{ with } (R^2_{adj} = 0.981)$$

The residuals for those fits are shown below:

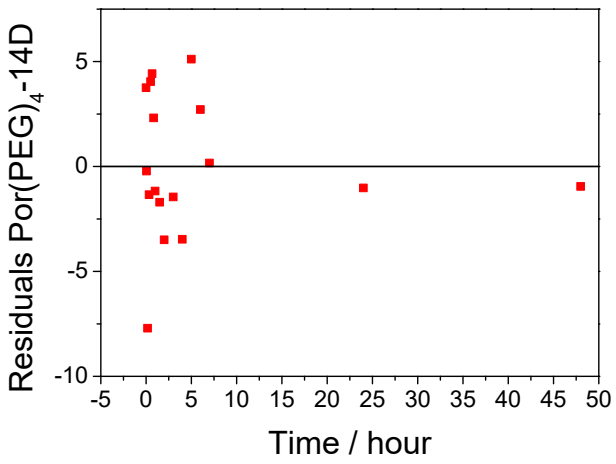

The results of the bi-exponential fit are summarized in the following table:

Table S1. Rate constants, k, contributions and maximum percentage of deuteration of the H/D exchange processes obtained after fitting the percentage of molecules with all hydrogen atoms exchanged for deuterium atoms with a bi-exponential growth function.

	Rate constants (h^{-1})		Maximum percentage of deuteration (%)
	k_{fast}	k_{slow}	
$Por(PEG)_4$	3.14	0.035	85.75

5. Singlet oxygen quantum yields (Φ_Δ)

Singlet oxygen quantum yields of **Por(PEG)$_4$** were measured in DMSO and D_2O following the well-known *relative method*, based on the photoinduced decomposition of a chemical trap based on 1,3-diphenylisobenzofuran (DPBF) in DMSO or 9,10-anthracenediyl-bis(methylene)dimalonic acid (ABDA) in D_2O, which easily reacts with $^1O_2$. TPP (Φ_Δ (DMSO) = 0.60) was used as the reference compound for the porphyrin in DMSO.[4] In water solution, the reference compound employed was Eosin Y (Φ_Δ (D_2O) = 0.60).[5]

The procedure was as follows: 2.5 mL of a stock solution of DPBF or ABDA (with an absorbance of approximately 1) in DMSO or D_2O was transferred to a 10 x 10 mm quartz optical cell and bubbled with oxygen for 1 min. A concentrated stock solution of **Por(PEG)$_4$** in

the same solvent was then added in a defined amount to achieve a final absorption value of the Q band of approximately 0.1. The solution was irradiated with stirring for defined time intervals, using a halogen lamp (300 W). The duration of these intervals was adjusted in each experiment in order to obtain a decrease in the absorption of DPBF or ABDA of about 3-4%. Incident light was filtered through a water filter (6 cm) and an additional filter to remove light below 530 nm (Newport filter FSQ-OG530). Additional neutral density filters (FBS-ND03 or FB-ND10) were used when necessary. The decrease in absorbance of DPBF or ABDA upon irradiation time was recorded at 414 and 399 nm respectively. Φ_Δ was calculated using the following equation:

$$\phi_\Delta^S = \phi_\Delta^R \frac{K^S I_{aT}^R}{K^R I_{aT}^S}$$

where *R* and *S* indicate the reference and sample, respectively. *K* is the slope obtained from the representation of ln (A_0/A_t) versus the irradiation time *t*, where A_0 and A_t are the absorbance of the chemical trap at the monitoring wavelength before and after the irradiation time *t*, respectively. I_{aT} is the total amount of light absorbed by the chromophore and is calculated as the sum of the intensities of the absorbed light I_a from wavelength 530 to 800 nm. I_a at the given wavelength is calculated using the Beer's law:

$$I_a = I_o\left(1 - e^{-2.3A}\right)$$

where *A* is the absorbance of the photosensitiser at the determined wavelength, and I_0 the transmittance of the filter at the same wavelength.

6. Calculation of fluorescence quantum yields (Φ_F)

The fluorescence quantum yields (Φ_F) were determined by comparing the properly integrated fluorescence intensity signal between solutions of the compounds to be studied and a solution of a reference compound by the method of Williams and co-workers.[6] For **Por(PEG)$_4$** the reference compound was TPP in DMSO (Φ_F = 0.11 ± 0.02).[7] When the reference is presented in another solvent than the sample, the fluorescence intensity is corrected according to the refractive index of the solvents used by applying the following equation:

$$\phi_F = \frac{A_S \cdot n_S^2}{A_R \cdot n_R^2}$$

where A_S and A_R are the areas corresponding to the sum of the intensities of the fluorescence band of the sample and the reference, respectively, and *n* is the refractive index of the solvent used. The excitation wavelength was set at 529 nm.

7. Cell lines and culture conditions

HeLa (ATCC, no. CCL-2) and HepG2 (ATCC, no. HB-8065) cells were obtained from ATCC and maintained in Dulbecco's modified Eagle medium (DMEM) supplemented with fetal bovine serum (10%) and penicillin-streptomycin (100 units mL^{-1} and 100 μg mL^{-1} respectively). All the cells were grown in a humidified incubator with 5% CO_2 at 37 °C.

8. Confocal laser scanning microscopy

Approximately 4 × 10^5 cells in DMEM (2 mL) were seeded on a confocal dish and incubated overnight at 37 °C with 5% CO_2. The cells were treated with the **Por(PEG)$_4$** supramolecular nanofibres. After that, the medium was removed, and the cells were rinsed with phosphate-buffered saline (PBS) and examined with a Leica TCS SP8 high speed confocal microscope. The excitation and emission wavelengths of porphyrin were 552 and 600–800 nm respectively.

9. Flow cytometry

Approximately 2 × 10^5 cells were inoculated into each of the wells in a 12-well plate and incubated in DMEM overnight at 37 °C and 5% CO_2. The cells were treated with the **Por(PEG)$_4$** supramolecular nanofibres. After that, the cells were rinsed with PBS and harvested by adding 0.5 mL of 0.25% trypsin–ethylenediaminetetraacetic acid (Invitrogen). After adding 0.5 mL of medium to quench the activity of the trypsin, the cell mixture was centrifuged at 1500 rpm for 3 min at room temperature. The cell pellet was washed with 1 mL of PBS and subject to centrifugation for three times. After resuspending the cells in 1 mL of PBS, their intracellular fluorescence intensities were measured by using a BD FACSVerse flow cytometer (Becton Dickinson) with 10^4 cells counted in each sample. Data collected were analysed by using the BD FAC-Suite. All experiments were performed in triplicate.

10. Subcellular localisation studies

Approximately 2 × 10^5 cells were seeded on a confocal dish and incubated overnight at 37 °C in a humidified 5% CO_2 atmosphere. The cells, after being rinsed with PBS, were incubated with the **Por(PEG)$_4$** supramolecular nanofibres ([Por] =20 μM) for 24 h. After being washed twice with PBS, the cells were stained with LysoTracker Green DND-26 (Thermo Fisher Scientific Inc., L7526) (2 μM), MitoTracker Green FM (Thermo Fisher Scientific Inc., M7514) (0.2 μM), or ER-Tracker Green (Thermo Fisher Scientific Inc., E34251) (1 μM) in a serum-free medium at 37 °C for 30, 15 and 15 min, respectively. The solutions were then removed, and the cells were rinsed with PBS twice before being examined with a Leica TCS SP8 high-speed confocal

microscope equipped with a 488 nm laser and a 638 nm laser. All the trackers were excited at 488 nm, and their fluorescence was monitored at 500−570 nm, while the porphyrin was excited at 552 nm and its fluorescence was monitored at 600−800 nm. The images were digitised and analysed using a Leica Application Suite X software.

11. *In vitro* cytotoxicity

Approximately 2 × 10^4 cells were inoculated into each of the wells in a 96-well plate and incubated in DMEM overnight at 37 °C and 5% CO_2. The cells were incubated with different concentrations of **Por(PEG)$_4$** supramolecular nanofibres for 24 h, and then were rinsed with 100 μL of PBS twice and replenished with 100 μL of fresh medium. For the dark cytotoxicity assay, the plate was directly incubated at 37 °C overnight. For the photocytotoxicity test, the cells were illuminated at room temperature for 20 min and then incubated overnight. The light source consisted of a 300 W halogen lamp, a water tank for cooling and a colour glass filter (Newport) cut on at λ = 515 nm. The fluence rate (λ ≥ 515 nm) was 25.5 mW cm^{-2}. Illumination for 20 min led to a total fluence of 30.6 J cm^{-2}. A solution of MTT (Sigma) in PBS (3 mg mL^{-1}, 50 μL) was added to each well. After incubation for 4 h under the same condition, 100 μL of DMSO was added to each well and the plates were placed on a Bio-Rad microplate reader to detect the absorbance at 490 nm. The average absorbance of the blank wells (not seeded with cells) was subtracted from the measured absorbance values of wells of various treatment groups. Cell viability was determined by the equation %viability = [∑(Ai/Acontrol × 100)]/n, where Ai is the absorbance of the ith datum (i = 1, 2, ..., n), Acontrol is the average absorbance of control wells in which the nanosystem was absent. The size of treatment group (n) is 4.

12. *In vivo* PDT efficacy

All experiments involving live animals were performed in strict accordance with the animal experimentation guidelines and were approved by the Animal Experimentation Ethics Committee of The Chinese University of Hong Kong (CUHK) (ref. no. 20-028-GRF). Licence to conduct animal experiments was obtained from the Department of Health, Government of the Hong Kong Special Administrative Region. Female Balb/c nude mice (20-25 g) were obtained from the Laboratory Animal Services Centre at CUHK. The mice were kept under a pathogen-free condition with free access to food and water. HeLa cells (5 × 10^7 cells in 200 μL) were inoculated subcutaneously on the back of the mice. Once the tumour volumes reached to ~60 mm^3, the mice were randomly divided into two groups: (1) with an intravenous injection of PBS

(200 μL) without laser irradiation, (2) with an intravenous injection of **Por(PEG)$_4$** followed by laser irradiation. The drug dose for **Por(PEG)$_4$** was 20 nmol in 200 μL of water. For the light-treatment group, the tumour was irradiated at 48 h post-injection with a diode laser (Biolitec Ceralas) at 675 nm operated at 0.6 W for 10 min, leading to a total fluence of 360 J cm^{-2}. The tumour volume as determined by the formula: Volume (mm^3) = (Length × Width^2)/2 was compared with that for the control group. On Day 14 after the treatment, the mice were sacrificed and the tumours were removed and weighed.

13. Synthetic procedure

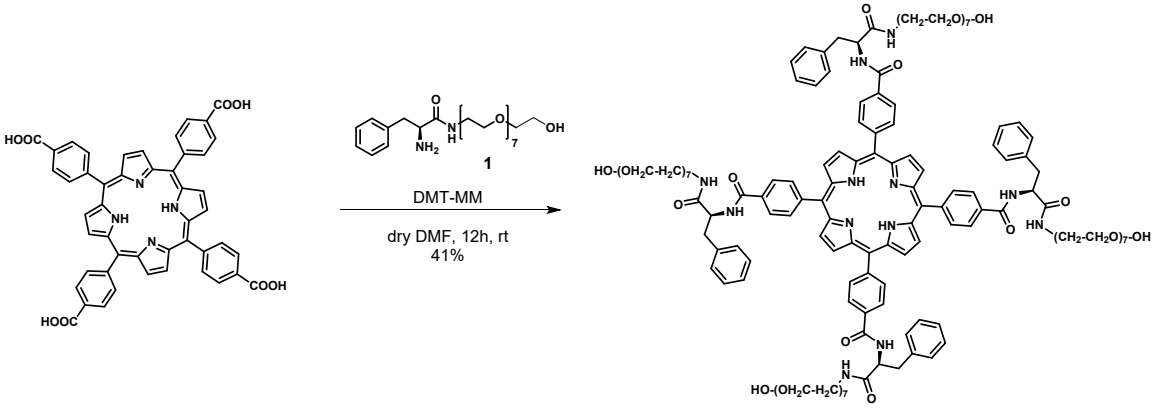

Scheme S1. Preparation of **Por(PEG)$_4$**.

Por(PEG)$_4$

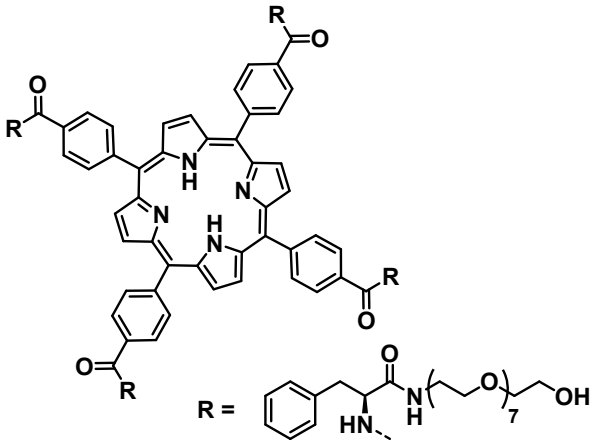

In a round bottom flask compound **1**[1] (0.10 g, 0.19 mmol) was added to a mixture of tetrakis(4-carboxyphenyl)porphyrin (0.02 g, 0.03 mmol) and DMTMM (4-(4,6-dimethoxy-1,3,5-triazin-2-yl)-4-methyl-morpholinium chloride) (0.07 g, 0.24 mmol) in THF (15 mL). Subsequently, the reaction mixture was stirred overnight under an argon atmosphere. The mixture was concentrated *in vacuo* and the residue was purified by column chromatography in silica gel with a mixture of chloroform and methanol (95/5 v/v) as eluent to afford **PorPEG$_4$** as a red oil (0.04 g, 0.013 mmol, 41%).

^{1}H NMR (300 MHz, $CDCl_3$, δ): 8.81 (s, 8 H, Por), 8.27 (m, *J* = 7.5 Hz, 8 H, Ar), 8.17 (m, *J* = 7.5 Hz, 8 H, Ar), 7.38-7.45 (m, 24 H, Ar and CONH), 6.79 (s, 4 H, CONH), 5.01-5.03 (m, 4 H, CH), 3.32-3.70 (m, 140 H, CH_2 and OH), -2.83 (s, 2 H, NH). **^{13}C NMR** (75 MHz, $CDCl_3$, δ): 171.04, 167.14, 145.55, 137.03, 134.77, 133.77, 129.70, 128.85, 127.21, 125.78, 119.49, 77.16, 72.69, 70.70, 70.63, 70.43, 69.78, 61.80, 55.36, 39.63, 39.26, 29.85. **MS** MALDI-TOF (DCTB): *m*/*z* 2807.3 (100%) $[M+Na]^+$. **HR-MS** MALDI-TOF (DCTB + PPGNa 2700): *m*/*z* calc for $C_{148}H_{198}N_{12}O_{40}$ $[M+Na]^+$: 2806.3702, found: 2087.3753.

^{1}H NMR spectrum of Por(PEG)$_4$ in $CDCl_3$

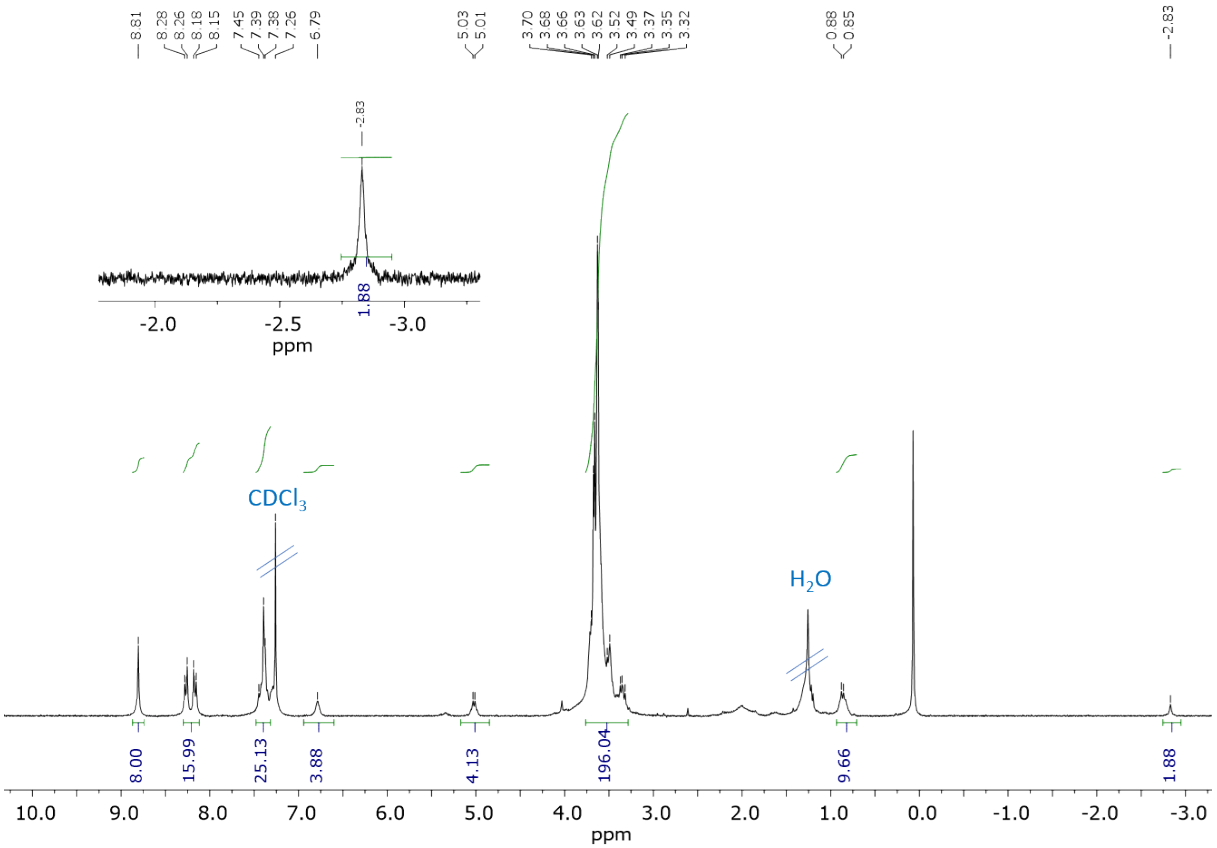

^{13}C NMR spectrum of Por(PEG)$_4$ in $CDCl_3$

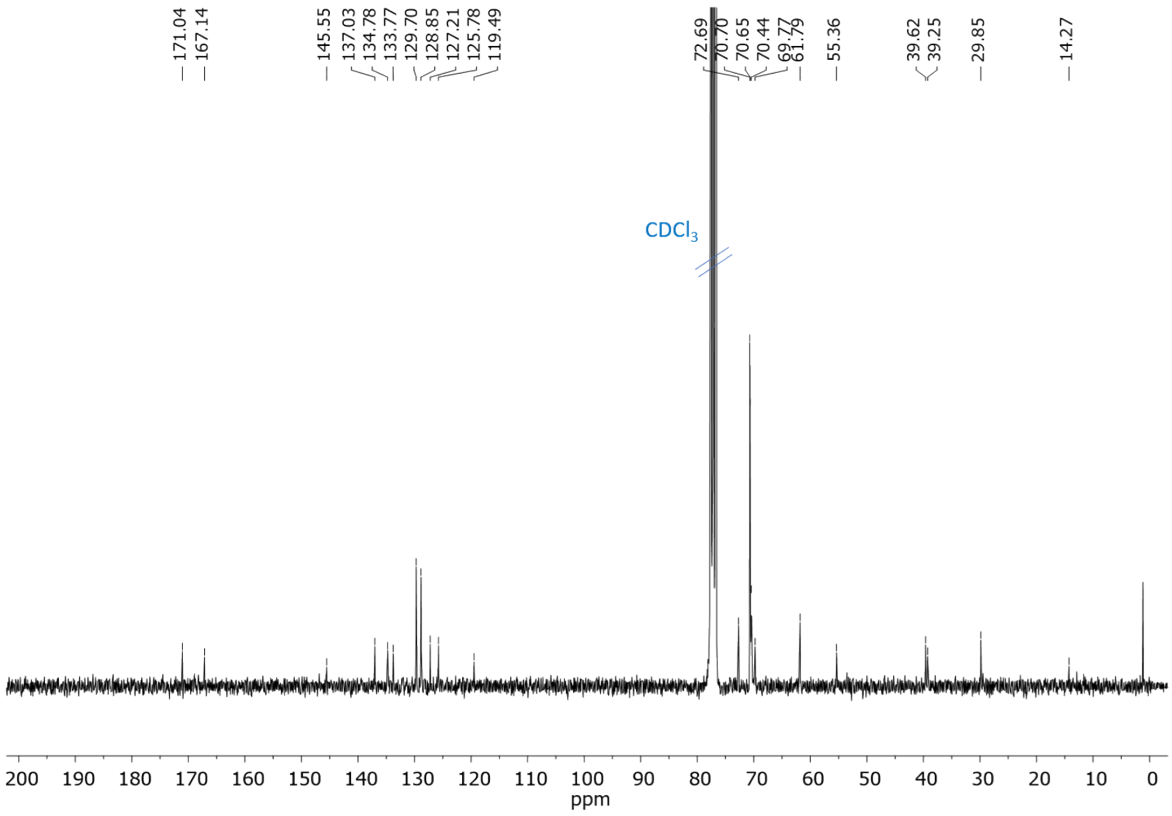

MALDI-TOF mass spectrum of Por(PEG)$_4$. The inset shows the experimental and simulated isotopic distribution patterns of the [M+Na]$^+$ ions.

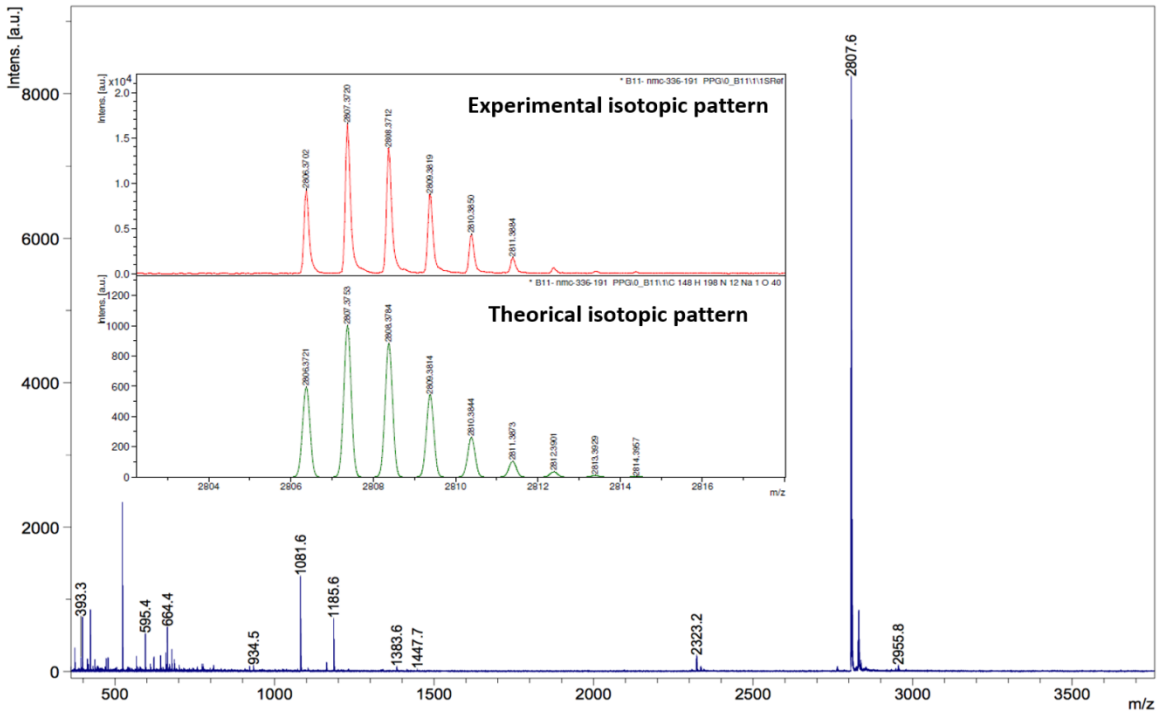

Supporting data

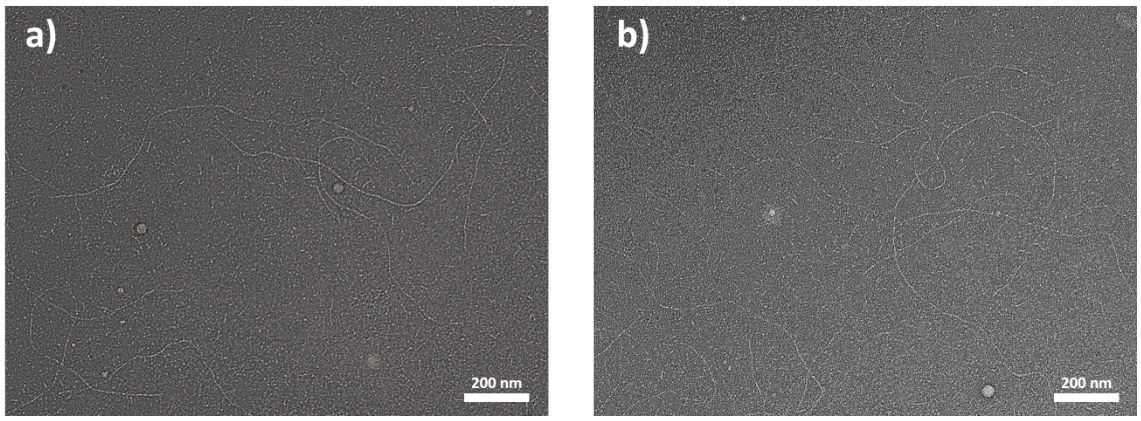

Fig. S1 TEM images of **Por(PEG)$_4$** in water using negative staining with uranyl acetate (2%) (c = 1 x 10^{-4} M).

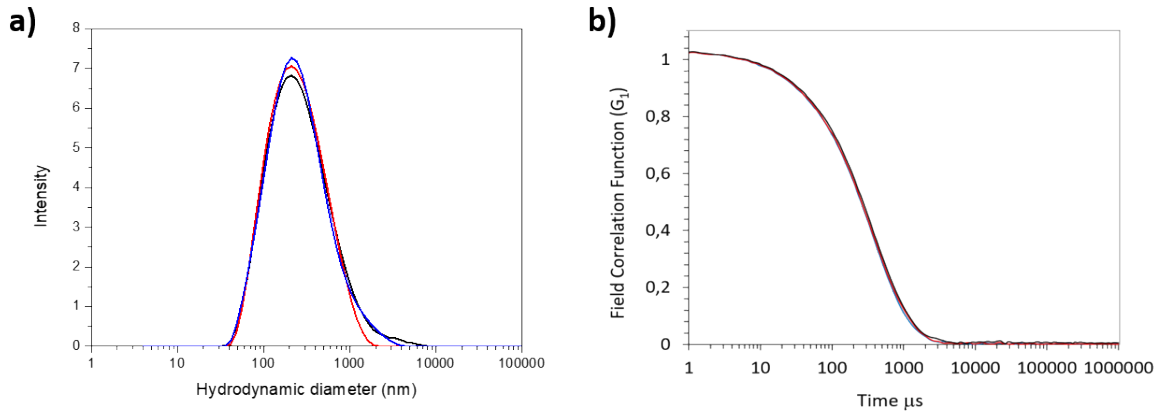

Fig. S2 (a) Hydrodynamic diameter distribution and (b) Correlogram of **Por(PEG)$_4$** in water measured by DLS . **Por(PEG)$_4$** was dissolved in 10 µL DMSO and diluted with 990 µL deionised water to a final concentration of 100 µM. The hydrodynamic diameter (385 ± 81 nm) is presented as the mean ± standard deviation (SD) of 3 independent consecutive measurements (the red, blue and black lines).

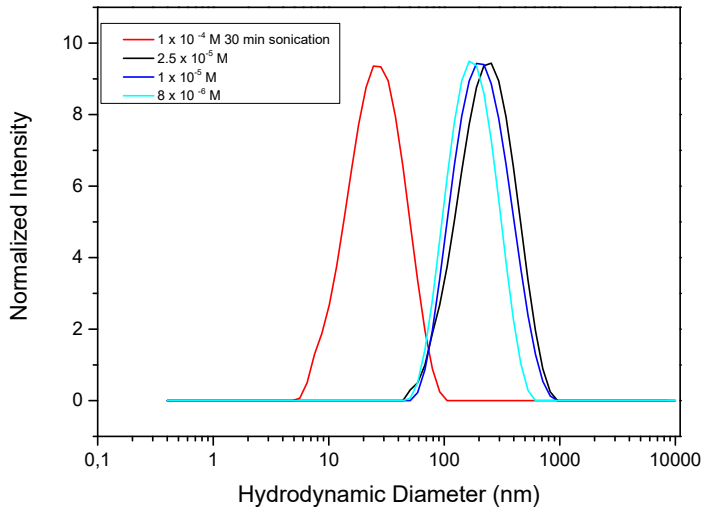

Figure S3: Hydrodynamic diameter distribution of **Por(PEG)$_4$** in water (c = 1 x 10^{-4} M). The averages values were: a) 255 nm with a polydispersity index (PDI) of 0.423 for a c = 2.5 x 10^{-5} M; b) 210 nm with a polydispersity index of 0.431 for a c = 1 x 10^{-5} M; c) 164 nm with a polydispersity index of 0.443 for a c = 8 x 10^{-6} M; d) 34 nm with a polydispersity index of 0.313 for a c = 1 x 10^{-4} M after 30 min of sonication.

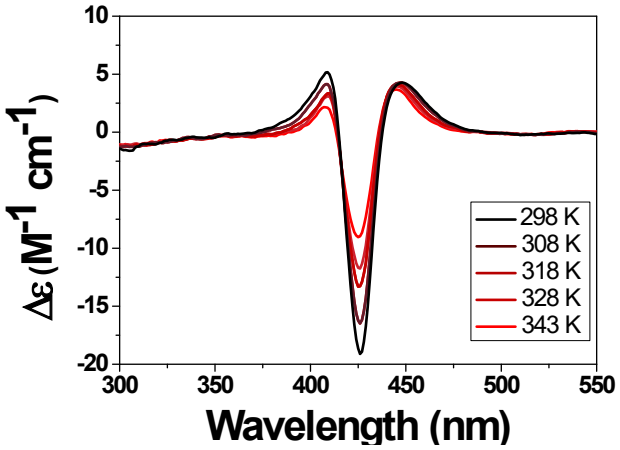

Fig. S4 Circular dichroism spectra of **Por(PEG)$_4$** in water at different temperatures between 293 K (black) and 343 K (red) (c = 2.5 x 10^{-5} M).

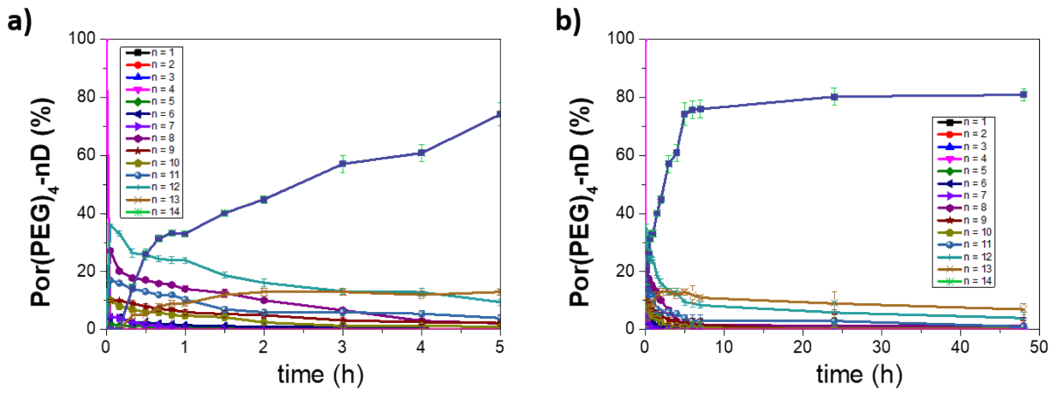

Fig. S5 Percentage of the different deuterated analogues of **Por(PEG)$_4$** as a function of time after 10x dilution of a 5.0 x 10^{-3} M sample into D_2O at room temperature. Data are reported as the mean ± SD of two independent measurements. (a) Zoom-in of the first 30 min of the HDX-MS experiments. (b) Zoom-out of the full HDX-MS experiments.

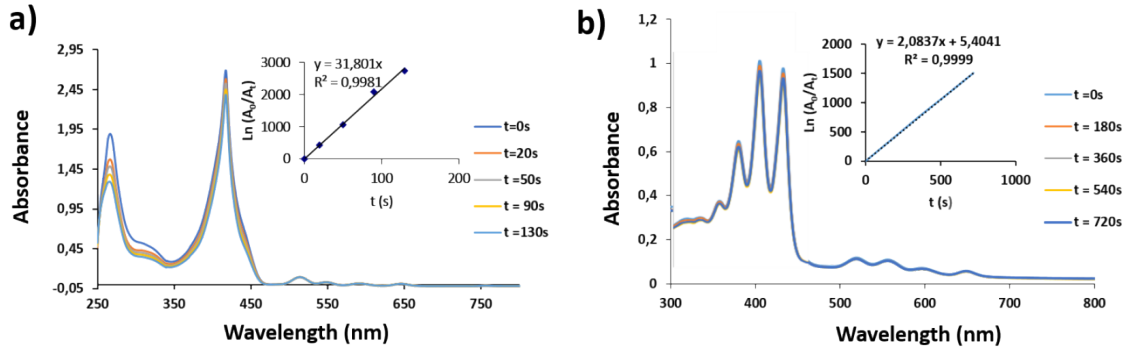

Fig. S6 Time-dependent photobleaching of (a) DBPF in DMSO and (b) ABDA in water in the presence of **Por(PEG)$_4$**, which is directly related to its $^1O_2$ generation efficiency.

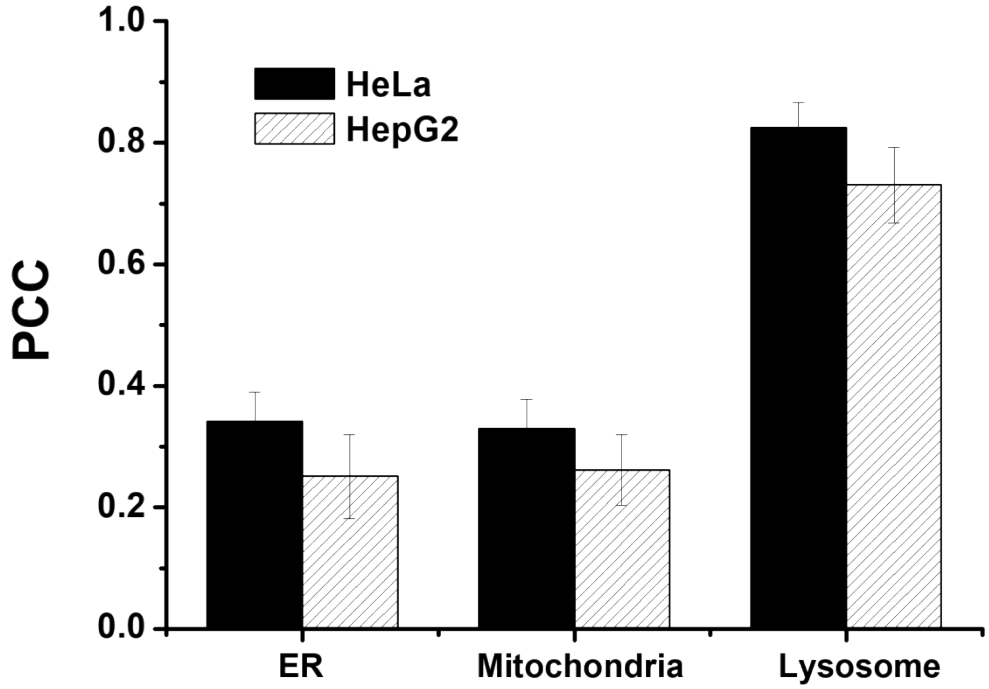

Fig. S7 Pearson's correlation coefficient (PCC) values for various subcellular trackers in HeLa and HepG2 cells. Data were obtained by analysing 50 cells and are presented as the mean ± SD of three independent measurements.

References

1. N. M. Casellas, S. Pujals, D. Bochicchio, G. M. Pavan, T. Torres, L. Albertazzi and M. García-Iglesias, *Chem. Commun.*, 2018, **54**, 4112.
2. P. A. Korevaar, C. Schaefer, T. F. A. de Greef and E. W. Meijer, *J. Am. Chem. Soc.*, 2012, **134**, 13482.
3. X. Lou, S. M. C. Schoenmakers, J. L. J. van Dongen, M. Garcia-Iglesias, N. M. Casellas, M. Fernández-Castaño Romera, R. P. Sijbesma, E. W. Meijer and A. R. A. Palmans, *J Polym Sci.* 2021, **59**, 1151.
4. W. Spiller, H. Kliesch, D. Wöhrle, S. Hackbarth, B. Röder and G. Schnurpfeil, *J. Porphyrins Phthalocyanines,* 1998, **2**, 145.
5. J. Y. Ma, M. I. Chen and T. J. Nyokong, *J. Phys. Chem. B.*, 2008, **112**, 15.
6. A. T. R. Williams, S. A. Winfield and J. N. Miller, *Analyst*, 1983, **108**, 1067.
7. S. Silva, P. M. R. Pereira, P. Silva, F. A. Almeida Paz, M. A. F. Faustino, J. A. S. Cavaleiro and J. P. C. Tomé, *Chem. Commun.,* 2012, **48**, 3608.